A phenomenological muscle model to assess history dependent effects in human movement

C.P. McGowan [a,*], R.R. Neptune [b], W. Herzog [c]

[a] Department of Biological Sciences, University of Idaho, Moscow, ID 84844, USA
[b] Department of Mechanical Engineering, University of Texas at Austin, Austin, TX 78712, USA
[c] Faculty of Kinesiology, University of Calgary, Calgary, Alberta, Canada T2N 1N4

ARTICLE INFO

ABSTRACT

Most musculoskeletal models used to analyze human movement utilize Hill-type muscle models that account for state dependent intrinsic muscle properties (e.g., force–length–velocity relationships), but rarely do these models include history dependent effects (e.g., force depression or enhancement). While the relationship between muscle shortening and force depression can be well characterized by muscle mechanical work, the relationship between muscle stretch and force enhancement is more complex. Further, it is not well known how these properties influence dynamic movements. Therefore, the goal of this study was to develop a modified Hill-type muscle model that incorporated stretch-induced force enhancement into a previously described model that included shortening-induced force depression. The modified muscle model was based on experimental data from isolated cat soleus muscles. Simulations of in situ muscle experiments were used to validate the model and simulations of a simple human movement task (counter-movement jumping) were used to examine the interactions of the history dependent effects. The phenomenological model of stretch-induced force enhancement was dependent on both the magnitude of stretch and relative length of the muscle fiber. Simulations of the in situ muscle experiments showed that the model could accurately reproduce force enhancement and force depression, as well as the complex additive relationship between these effects. Simulations of counter-movement jumping showed that a similar jump pattern could be achieved with and without history dependent effects and that a relatively minor change in muscle activation could mitigate the impact of these effects.

© 2012 Elsevier Ltd. All rights reserved.

1. Introduction

The effect of muscle length changes on its ability to generate isometric force is well documented. Generally referred to as history dependent effects, several studies have shown that the isometric force produced by a muscle following active shortening is reduced relative to an isometric contraction at the same length with no prior shortening (e.g., Abbott and Aubert, 1952; Herzog et al., 2000; Marechal and Plaghki, 1979). Conversely, muscles that are actively stretched produce higher isometric forces relative to muscles that were not stretched (e.g., Abbott and Aubert, 1952; Edman et al., 1982; Herzog and Leonard, 2002; Hisey et al., 2009). To date, the majority of these studies have focused on characterizing the relationships between the history of muscle length change and the resulting isometric force.

Shortening-induced force depression has been shown to be correlated with both the magnitude (e.g., Edman, 1975; Marechal and Plaghki, 1979) and rate (e.g., Marechal and Plaghki, 1979; Meijer et al., 1998) of shortening; although Herzog and Leonard (1997) showed that force depression may be independent of velocity if the force remains constant during shortening. More recently, studies have shown that force depression is strongly correlated with the amount of mechanical work the muscle does during shortening (Herzog et al., 2000; Josephson and Stokes, 1999; Kosterina et al., 2008). The relationship between the time history of active stretch and force enhancement appears to be more complex. Force enhancement does not correlate with a simple scalar quantity such as muscle work, and the position of the muscle on the force length curve during stretch may have a substantial impact on the magnitude of force enhancement (Bullimore et al., 2007; Edman et al., 1978; Hisey et al., 2009). On the descending limb of the force–length curve, the magnitude of force enhancement is directly related to the length of the stretch (e.g., Abbott and Aubert, 1952; Bullimore et al., 2007; Edman et al., 1978; Hisey et al., 2009). However, stretches ending

* Correspondence to: Department of Biological Sciences, Life Sciences, South Moscow, ID 84844-3051, USA. Tel.: +1 208 885 6598.
E-mail address: cpmcgowan@uidaho.edu (C.P. McGowan).

on the ascending limb and plateau region of the force–length curve produce relatively small amounts of force enhancement and are largely independent of the stretch length (e.g., Hisey et al., 2009; Lee et al., 2001; Peterson et al., 2004). Studies have also shown that force depression and force enhancement are cumulative when a muscle shortens before stretching, but not when a muscle is first stretched and then shortened (e.g., Herzog and Leonard, 2000; Lee et al., 2001).

Based on these empirical relationships, a number of studies have developed phenomenological models that incorporate history dependent effects into their estimates of force output (e.g., Ettema, 2002; Ettema and Meijer, 2000; Forcinito et al., 1998; Meijer et al., 1998; Williams, 2010). Of the studies that do include history dependent effects, few have used the models to examine their influence on dynamic movements (Ettema, 2002; Williams, 2010). In a recent study, we developed and validated a modified-muscle model that included shortening-induced force depression based on the relationship with mechanical work (McGowan et al., 2010). The study showed that in maximal power pedaling, force depression has the potential to substantially reduce the amount of crank power that is produced by muscles. However, it is not clear to what extent force enhancement effects mechanical output, nor is it known to what degree force depression and force enhancement offset one another during cyclic movements.

Therefore, the goal of this study was to develop a modified Hill-type muscle model that included both stretch-induced force enhancement and shortening-induced force depression that can be incorporated into a forward dynamics simulation to examine the influence of these history dependent effects on human movement. We first developed and validated a modified-muscle model that incorporated both stretch-induced force enhancement and force depression. The model's accuracy was evaluated by comparing the outputs from simulated in situ experiments with actual experimental data from isolated cat soleus muscles. We then used the model in a simulated countermovement jumping task to assess the influence of history dependent effects on human movement performance.

2. Methods

2.1. Force enhancement model

The force enhancement model consisted of a modified Hill-type model (Zajac, 1989) with three components (Fig. 1). Residual force enhancement (FE_{res}) is the long lasting component that appears as the difference in isometric force following an active stretch and the isometric reference force (i.e., with no previous length change). Dynamic force enhancement (FE_{dyn}) occurs when the muscle is being stretched and transient force enhancement (FE_{trans}) is the delay in return to steady-state force following the end of the stretch. The total force enhancement (FE_{total}) is equal to FE_{dyn} during the stretch and the sum of FE_{res} and FE_{trans} following the stretch, which is added to the force calculated from the standard Hill-type model. FE_{total} was set to zero prior to active stretching or when the muscle begins to shorten.

Based on experimental data from cat soleus muscles, when a muscle is actively stretched on the descending limb of the force–length curve, the relationship between FE_{res} (normalized to maximal isometric force) and muscle length change (ΔL) is best described by a second order polynomial equation ($R^2 > 0.99$) such that

$$FE_{res} = a\Delta L_i^2 + b\Delta L_i + c, \quad \text{if } L_i > 1.0 \tag{1a}$$

where L_i is the current length of the muscle normalized by the muscle's rest length (L_0). Values for the constants were taken from the average of three experimental stretch velocities (3 mm/s, 9 mm/s and 27 mms/s) and were -2.00, 1.10 and 0.00 for a, b and c, respectively. Previous work has shown that active stretches over a threshold value of $\sim$25% of fiber length no longer result in increased force enhancement (Hisey et al., 2009). Therefore, when stretches exceed 25% of L_0, ΔL was held constant at that length for the calculation of force enhancement. On the ascending limb of the force–length curve, FE_{res} was considered to be independent of length change and equal to 3% or 1% of muscle force if L_i was between 85% and 100% or less than 85% of L_0, respectively (Lee et al., 2001;
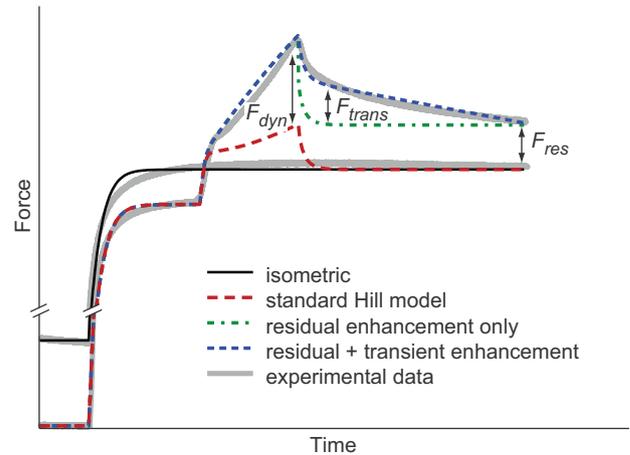

Fig. 1. A schematic showing the components of the history dependent stretch force enhancement model. The model including residual force enhancement (F_{res}), transient force enhancement (F_{trans}) and dynamic force enhancement (F_{dyn}) provides the best match with experimental data. For comparison, the force produced by a classic Hill-type model undergoing the same active stretch is shown.

Hisey et al., 2009). FE_{res} was calculated as:

$$FE_{res} = F_i * 0.03, \quad \text{if } 0.85 < L_i < 1.0 \tag{1b}$$

$$FE_{res} = F_i * 0.01, \quad \text{if } L_i < 0.85 \tag{1c}$$

where F_i is the current muscle force. In order to avoid discontinuities, FE_{res} increased by the same relationship as on the descending limb until the target 3% or 1% was reached.

Previous studies have shown force enhancement during the stretch is correlated with the magnitude of the residual force enhancement (Edman and Tsuchiya, 1996), thus FE_{dyn} was calculated as:

$$FE_{dyn} = FE_{res} * 2.0 \tag{2}$$

At the end of the active stretch, FE_{trans} was calculated based on experimental data from the cat soleus muscle (Herzog and Leonard, 2002) as:

$$FE_{trans} = A + kt \tag{3}$$

where A is the difference between FE_{dyn} and FE_{res} at the end of the stretch and t is the time from the end of the stretch. The transient period of force enhancement is terminated by setting FE_{trans} to zero when the value for Eq. (3) becomes negative. The value for k was also based on experimental data and was calculated as:

$$k = a\Delta L_i^2 + b\Delta L_i + c \tag{4}$$

where a, b and c were equal to 9.61, -5.44 and 0.00, respectively.

Total force enhancement was determined using the equation:

$$FE_{total} = \begin{cases} FE_{dyn}, & \text{when } vel_{MTU} > 0 \\ FE_{res} + FE_{trans} & \text{when } vel_{MTU} = 0 \text{ following a stretch} \\ 0 & \text{when } vel_{MTU} < 0 \end{cases} \tag{5}$$

2.2. Force depression model

The force depression model has been described previously in detail (McGowan et al., 2010). Briefly, the total force depression (FD_{total}) is the sum of static force depression, based on the work done during shortening, and transient force depression, described by an exponential term which is also a function of net muscle work. Force depression is long lasting and persists until the muscle is deactivated.

2.3. Combined muscle model

The standard Hill-type model, and force enhancement and force depression models were combined to predict force based on the muscle's current state and fiber length change history. Because force enhancement was abolished as soon as the muscle begins to shorten, the effects were not cumulative in stretch–shorten cycles. However, because force depression was maintained until the muscle was deactivated, the effects were cumulative in shorten–stretch cycles. The total force

produced by the combined modified-muscle model was calculated as:

$$F' = F_i + FE_{total} - FD_{total} \qquad (6)$$

2.4. Single muscle in situ simulations

To validate the muscle model's ability to reproduce empirical measurements of whole muscle force enhancement, a muscle ergometer model (McGowan et al., 2010) was used to simulate a subset of the experimental protocol from Herzog and Leonard (2002). Their experiments compared the isometric force following constant velocity stretches of active muscles with the isometric force of a muscle that was not stretched. Individual stretches were made for three lengths (3 mm, 6 mm and 9 mm) at three different velocities (3 mm/s, 9 mm/s and 27 mm/s) for a total of nine stretches. Isometric contractions and all stretches ended at rest length +9 mm. Optimal muscle fiber length (36 mm), tendon slack length (74 mm, including aponeurosis), maximum shorting velocity (3.3 lengths/sec) and maximum isometric force (28.6 N) were set to approximate the average values for cat soleus muscles (Herzog and Leonard, 2002). In a second set of simulations, the ergometer model was used to examine the model's ability to reproduce experimental data from sequential stretch–shorten and shorten–stretch cycles (Fig. 3). The magnitudes and rates of length change were based on the experiments of Herzog and Leonard (2000) to facilitate comparisons to data in the literature (Herzog and Leonard, 2000; Lee et al., 2001).

2.5. Countermovement jumping simulation

To assess the effect of history dependent properties on human movement performance, simulations of countermovement jumping were generated with and without the modified-muscle model. The simulations used a previously described (e.g., McGowan et al., 2009; Neptune et al., 2009) detailed musculoskeletal model (Fig. 4) developed using SIMM/Dynamics Pipeline (MusculoGraphics, Inc.) and the equations of motion were generated using SD/FAST (PTC). Muscle excitations were modeled using the sum of four Henning patterns, each with three parameters (onset, offset, magnitude) for a total of 12 parameters per muscle (Rankin et al., 2011). Foot–ground contact was modeled using 30 viscoelastic elements with Coulomb friction on the plantar surface of the three foot segments (Neptune et al., 2000).

To generate the countermovement simulations, the initial conditions and excitation patterns were optimized using a simulated annealing algorithm (Goffe et al., 1994). A starting guess for the initial conditions (static standing with slightly flexed legs) and excitation patterns was based on our experimental data and electromyography data taken from the literature (Voigt et al., 1995). A control simulation was generated using the standard Hill-type muscle model by minimizing the difference between simulated and experimental countermovement jump data (i.e., joint angles, hip height and ground reaction forces). A second simulation was generated using the modified-muscle model that minimized the differences between the simulated data using the modified-muscle model and the control simulation data.

2.6. Experimental data

Countermovement jumping data were collected at the University of Idaho using an IRB approved protocol. Ground reaction forces and kinematic data were measured using an in-ground force plate and 3D motion capture system. 16 retro-reflective markers were affixed with double-sided tape to specific landmarks according to the Modified Helen Hayes Marker set described by Kadaba et al. (1990). Three-dimensional positions of each marker were captured at 250 Hz via a Vicon MX motion analysis system (Vicon, Oxford Metrics Ltd., UK) and marker trajectory data were filtered using a Woltring filtering routine (Woltring, 1978). The ground reaction force (GRF) data were captured at 1000 Hz from the force plate in synchrony with the motion capture data. Force plate data were low-pass filtered at 30 Hz using a second-order Butterworth filter before being down sampled and combined with the motion capture data. Vicon Plug-in Gait was used to calculate the representative data required for the simulations. Data were the average of 10 trials from a single female subject (height—1.62 m, mass—71.2 kg) who provided her informed consent. The data were normalized by body mass and leg length to facilitate the comparison between the subject and the model.

3. Results

3.1. In situ muscle ergometer simulations

On the descending limb of the force–length curve, simulations of single muscle active stretches accurately reproduced experimental data for all conditions (Fig. 2). The average root mean square error (RMSE) between the simulations and experimental data while the muscle was active was 0.59 N (range: 0.45–0.85 N) for 3 mm/s stretches, 0.60 N (range: 0.36–1.05 N) for 9 mm/s stretches and 0.98 N (range: 0.68–1.42 N) for 27 mm/s stretches. Across all simulations, the average RMSE was 0.72 N. Using the Hill-type model alone resulted in an average RMSE of 4.41 N (range: 2.62–5.86 N) across all conditions.

Simulations of the stretch–shorten and shorten–stretch cycles were consistent with experimental data (Herzog and Leonard, 2000; Lee et al., 2001) and had an average RMSE of 2.41 N (range: 1.90–2.95 N). However, this was largely because the experimental data had a slightly higher isometric force than the model. When the model forces were adjusted such that the isometric force matched that of the experimental data, the RMSE was reduced to 0.74 N (range: 0.09–1.11 N). Thus, the model was able to reproduce the cumulative effects of force depression and enhancement
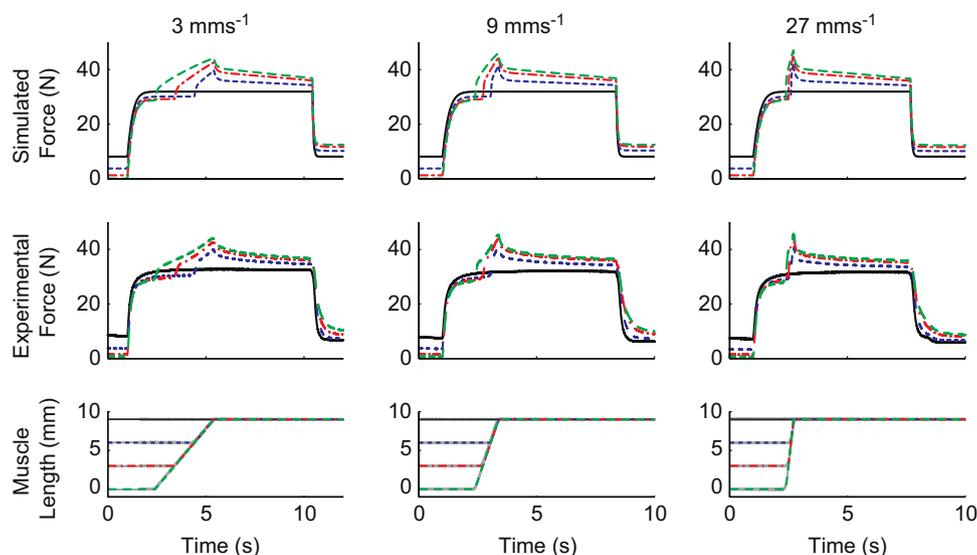

Fig. 2. A comparison of simulated and experimental in situ active stretch force data. Muscles were stretched over three different lengths (3, 6, and 9 mm) at three different speeds (3, 9 and 27 mm s^{-1}). The simulated force outputs (top row) agreed well with experimental force data (middle row) in all conditions. The individual colors and patterns within each column correspond to a given trial. The experimental data are average data from cat soleus muscles taken from Leonard and Herzog (2002).
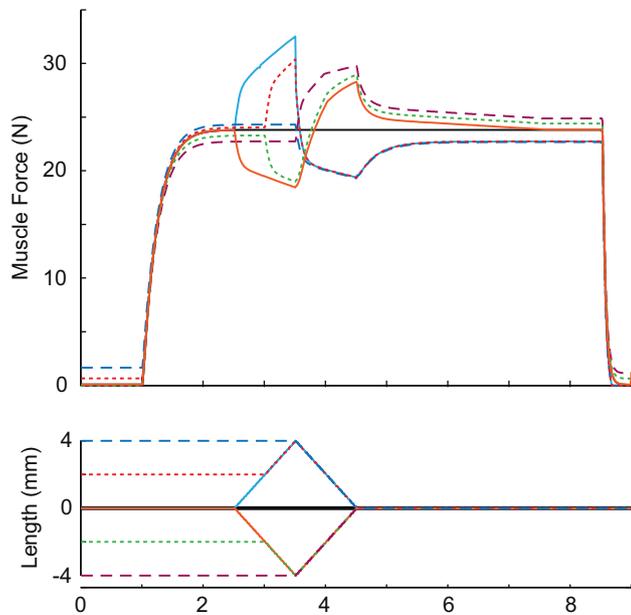
Fig. 3. Simulated force data from the modified muscle model for active stretch–shorten and shorten–stretch cycles. Stretch–shorten cycles consisted of 4 mm contractions preceded by active stretches of 0 mm, 2 mm and 4 mm. Shorten–stretch cycles consisted of 4 mm stretches preceded by contractions of 0 mm, 2 mm and 4 mm. All length changes occurred at 4 mm/s and ended at the muscle's optimal length. The modified muscle model includes both stretch induced force enhancement and shortening induced force depression. Colors and line patterns are the same for muscle force and length for each condition. Consistent with experimental data, history dependent effects are cumulative during shorten–stretch cycles but not during stretch–shorten cycles.

when the muscle underwent shorten–stretch cycles and the non-cumulative effects during stretch–shorten cycles (Fig. 3).

3.2. Countermovement jumping

The simulation incorporating the modified-muscle model was able to reproduce the jumping motions generated by the control simulation, which generally agreed well with experimental data (Fig. 5). The RMSE between the ground reaction forces, joint angles and hip height from the control simulation and the experimental data were 0.066BW, 5.5°, and 0.043 m, respectively; whereas the RMSE between the ground reaction forces, joint angles and hip height from the modified-muscle simulation and the control simulation were 0.053BW, 2.4°, and 0.005 m, respectively. The largest discrepancy between the data occurred in the horizontal ground reaction forces (Fig. 5), in which the simulated forces fluctuated around zero and did not match the pattern from the experimental data. However, these forces are quite small and likely do not contribute meaningfully to the predominately vertical jumping task. Rather, they likely reflect the simulations trying to maintain fore–aft balance without the feedback present in biological legs.

The uni-articular soleus, vastus lateralis and gluteus maximus were chosen to examine the effects of history dependent properties because they undergo the greatest length changes during the countermovement jump (Fig. 6). Soleus muscle activation patterns were nearly identical between the two simulations (Fig. 6A). Early active stretching of the soleus (Fig. 6B) produced a short duration force enhancement of 761 N (Fig. 6C), whereas rapid shortening before toe-off resulted in relatively little force depression (245 N). However, there was not a substantial effect on the total force produced during the upward acceleration phase of the jump. The vastus lateralis underwent a large stretch–shorten cycle, but was only active during a portion of the stretch
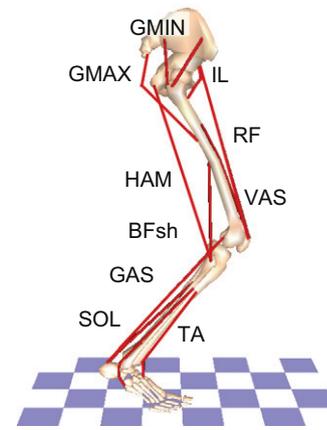

Fig. 4. The musculoskeletal model for simulations of countermovement jumping (right side shown) consisted of rigid segments representing the trunk and two legs, with each leg consisting of a thigh, shank, patella, and three-part foot for a total of 13° of freedom (flexion/extension at the hip, knee, ankle, mid-foot and toes of each leg along with vertical and horizontal translation and rotation of the trunk). The model was driven by 25 musculotendon actuators per leg grouped into 13 muscle groups based on anatomical function: IL (illiacus, psoas), GMAX (gluteus maximus, adductor magnus), GMED (anterior and posterior regions of the gluteus medius), VAS (3-component vastus), RF (rectus femoris), HAM (medial hamstrings, biceps femoris long head), BFsh (biceps femoris short head), GAS (medial and lateral gastrocnemius), SOL (soleus, tibialis posterior), TA (tibialis anterior, peroneus tertius), PR (peroneus longus, peroneus brevis), FLXDG (flexor digitorum longus, flexor hallucis longus) and EXTDG (extensor digitorum longus, extensor hallucis longus). PR, FLXDG, and EXTDG are not shown. Each muscle within a group received the same excitation pattern.

compared to all of the shortening (Fig. 6D,E). The active stretch produced a force enhancement of 536 N, and the active shortening produced 596 N of force depression (Fig. 6F). The gluteus maximus was active throughout the jump motion; however, the activation patterns differed substantially between the two simulations (Fig. 6G). The active stretch of the muscle began on the ascending limb of the force–length curve and continued well onto the descending limb (Fig. 6H), producing 676 N of force enhancement (Fig. 6I). Because the magnitude of the stretch exceeded 25% of the muscle's rest length, force enhancement reached a plateau for much of the stretching phase. The subsequent active shortening produced 449 N of force depression which was partially offset by higher muscle activation.

4. Discussion

The goal of this study was to develop a phenomenological muscle model that could reproduce both shortening-induced force depression and stretch-induced force enhancement. The simulation results show that the modified-muscle model was able to effectively reproduce both the magnitude and timing of history dependent effects measured during in situ stretch–shorten and shorten–stretch cycles. These results are consistent with previous phenomenological models that include both force depression and force enhancement (e.g., Ettema and Meijer, 2000; Forcinito et al., 1998). However, our model was also able to reproduce the cumulative effects which sum during shorten–stretch cycles but not during stretch–shorten cycles (Fig. 3), which some previous models could not account for (e.g., Forcinito et al., 1998). The influence of these effects on dynamic human movement was assessed during a countermovement jumping task. The jumping task showed that for a given excitation pattern, history dependent muscle properties have the capacity to substantially alter the timing and magnitude of muscle force production, which can result in changes in movement dynamics. However, when the muscle activation patterns were re-optimized,
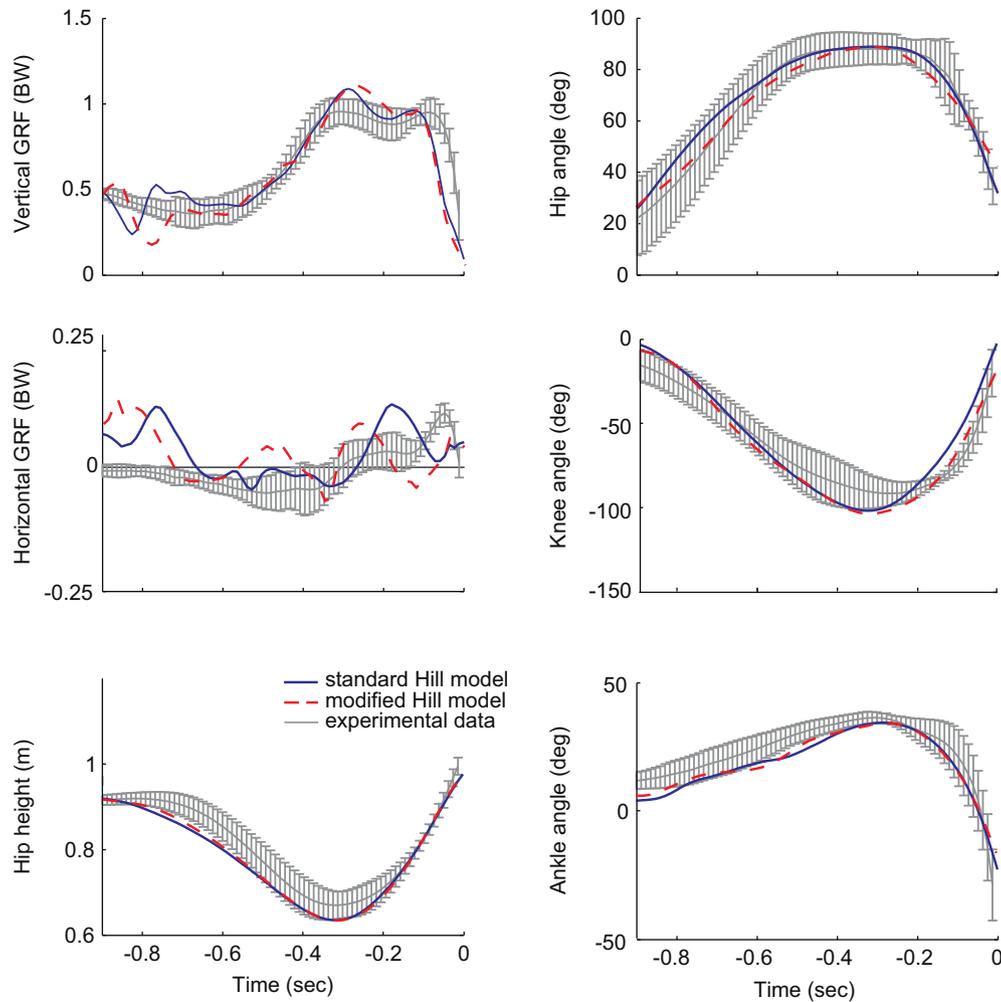
Fig. 5. Ground reaction force and kinematic data from the counter movement jump. The gray lines are the average experimental data ($\pm$ 2 standard deviations) from 10 jumping trials from a single subject. The solid blue lines are data from the control simulation and the dashed red lines are data from simulation with the modified muscle model. (For interpretation of the references to color in this figure legend, the reader is referred to the web version of this article.)

similar movement patterns were achieved with the modified-muscle model and standard-muscle model.

One of the outcomes of this study was to determine to what extent history dependent force enhancement and force depression offset one another in dynamic movement tasks. We found that in the countermovement jump (Fig. 6) the magnitudes of force enhancement and force depression were very similar. The force produced by each muscle was also affected by other factors. For example, slight differences in the joint motions meant that the muscle fibers were at slightly different states, and therefore other intrinsic properties (e.g., force–length, force–velocity) influenced the force output. Because the simulations were optimized independently, differences in muscle excitation patterns made it challenging to interpret isolated effects of individual history dependent properties. To control for this, we ran the modified-muscle model jumping simulation without allowing it to re-optimize muscle excitation patterns. However, this simulation did not result in a jumping motion.

The results of the countermovement jump simulation highlight the range of effects possible with the modified-muscle model (Fig. 6). The soleus experienced relatively small effects from history dependent properties, mainly because the muscle was active for only a short time during stretching and was not fully active until the end of the jump. This timing is generally consistent with experimental measurements of muscle activity during countermovement jumps (Voigt et al., 1995). The amount

of force depression that was developed while soleus was active was low because the muscle did relatively little work due the rapid drop in force during shortening, which was due in large part to the force–velocity relationship. The vastus lateralis was also only active for part of the stretch phase. The stretch-induced force enhancement and slight increase in muscle activation resulted in a peak force that was 22% higher, but changes in activation timing produced overall muscle force impulse that was 28% lower. Finally, the gluteus maximus was active throughout the stretch–shorten cycle and thus showed the greatest effects of history dependent properties. The active stretch was so great that it exceeded the threshold for which force enhancement has been shown to continue to increase (Hisey et al., 2009), and thus force enhancement plateaued and accounted for over half of the force produced during this period.

The aim of this study was to develop a relatively simple phenomenological muscle model that includes both force depression and enhancement effects and can be incorporated into complex musculoskeletal models and forward dynamic simulations. While our model achieved this aim, there are some limitations. Most notably, as a muscle actively stretches from the ascending limb onto the plateau and descending limb of the force length curve, the force enhancement increases instantaneously. Further, when the muscle transitions from stretching to shortening, the force enhancement rapidly disappears. These discontinuities in force, which are not present in biological systems,
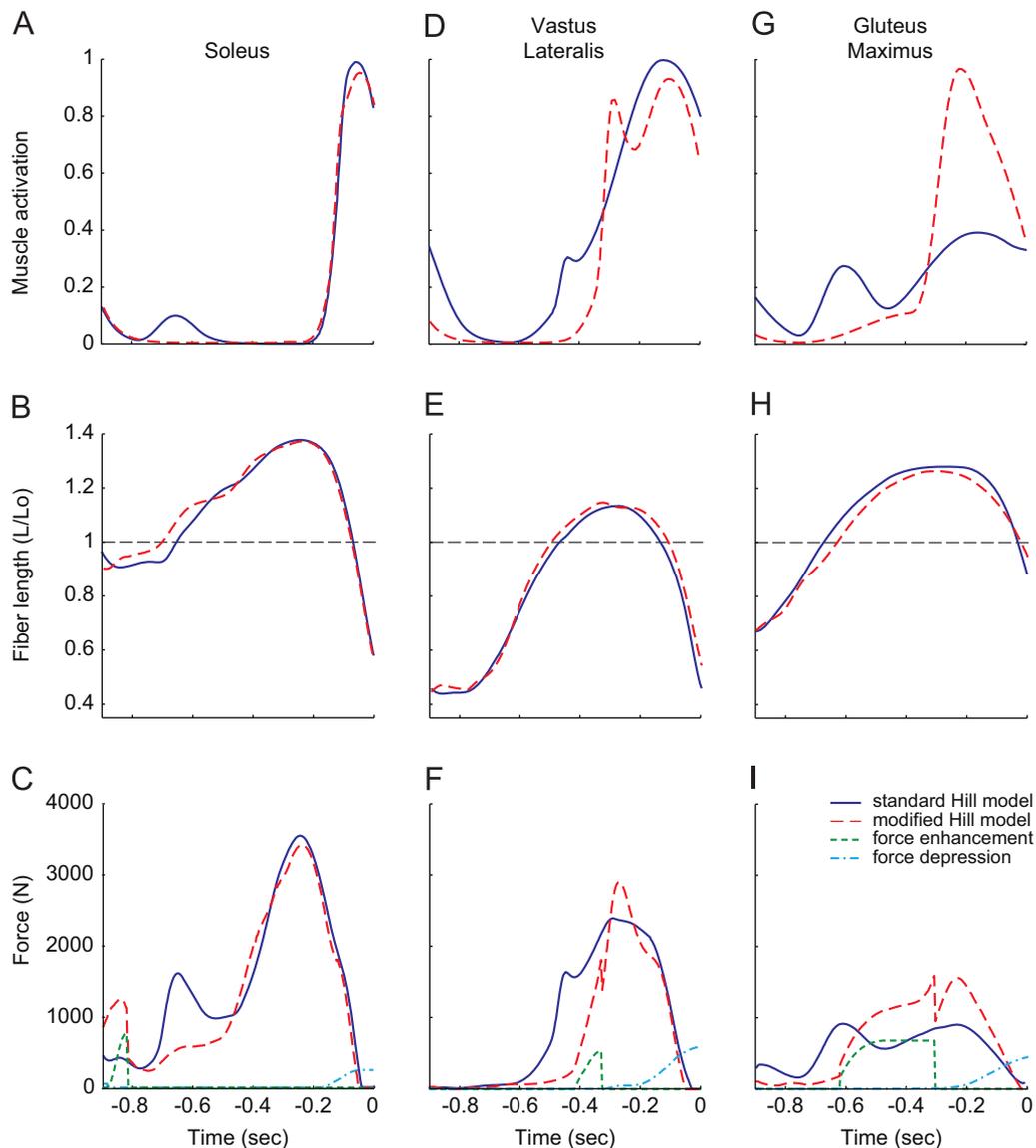
Fig. 6. Simulated muscle data for the soleus, vastus lateralis and gluteus maximus from the control simulation (solid lines) and simulation with the modified-muscle model (dashed lines). Muscle activation patterns (top row) were allowed to vary between the two simulations. Slight differences in kinematics produced small differences in muscle length change (middle row). The magnitude of force generated by muscles with the modified-muscle model included both stretch-induced force enhancement and shortening-induced force depression.

appear in our simulations because each muscle in the musculos-keletal model is modeled as a single fiber. During the transition from stretching to shortening in a whole muscle, the timing of the transition for each fiber making up the muscle will be slightly offset, effectively damping out any transient forces. However, as a result of these abrupt changes, the numerical integration of the equations-of-motion for the simulation becomes very stiff, thereby increasing the time for each simulation by as much as 10-fold. This means that the time required for optimization of more complex movements involving multiple muscle groups may become prohibitively long. Despite this limitation, the modified-muscle model developed here was able to elucidate the influence of history dependent effects during a relatively simple dynamic movement task. And while future modifications to this model that eliminate discontinuities in force production may enable it to be used in more complex simulations, our results suggest that in most submaximal activities, history dependent effects will likely be compensated for by changes in muscle excitation. For example, incorporation of the modified-muscle model into simulations of more complex movement tasks (e.g., slow running) produced

stable simulations. The results of these simulations were consistent with our finding for counter-movement jumping in that history dependent effects were compensated for by changes in muscle activation and had little impact on movement dynamics.

Conflict of interest statement

The authors have no conflict of interest.

Acknowledgments

References

Abbott, B.C., Aubert, X.M., 1952. The force exerted by active striated muscle during and after change of length. Journal of Physiology 117, 77–86.

Bullimore, S.R., Leonard, T.R., Rassier, D.E., Herzog, W., 2007. History-dependence of isometric muscle force: effect of prior stretch or shortening amplitude. Journal of Biomechanics 40, 1518–1524.

Edman, K.A., 1975. Mechanical deactivation induced by active shortening in isolated muscle fibres of the frog. Journal of Physiology 246, 255–275.

Edman, K.A., Elzinga, G., Noble, M.I., 1978. Enhancement of mechanical performance by stretch during tetanic contractions of vertebrate skeletal muscle fibres. Journal of Physiology 281, 139–155.

Edman, K.A., Elzinga, G., Noble, M.I., 1982. Residual force enhancement after stretch of contracting frog single muscle fibers. Journal of General Physiology 80, 769–784.

Edman, K.A., Tsuchiya, T., 1996. Strain of passive elements during force enhancement by stretch in frog muscle fibres. Journal of Physiology 490, 191–205.

Ettema, G.J., 2002. Effects of contraction history on control and stability in explosive actions. Journal of Electromyography and Kinesiology 12, 455–461.

Ettema, G.J., Meijer, K., 2000. Muscle contraction history: modified Hill versus an exponential decay model. Biological Cybernetics 83, 491–500.

Forcinito, M., Epstein, M., Herzog, W., 1998. Can a rheological muscle model predict force depression/enhancement? Journal of Biomechanics 31, 1093–1099.

Goffe, W.L., Ferrier, G.D., Rodgers, J., 1994. Global optimization of statistical functions with simulated annealing. Journal of Econometrics 60, 65–99.

Herzog, W., Leonard, T.R., 1997. Depression of cat soleus-forces following isokinetic shortening. Journal of Biomechanics 30, 865–872.

Herzog, W., Leonard, T.R., 2000. The history dependence of force production in mammalian skeletal muscle following stretch–shortening and shortening–stretch cycles. Journal of Biomechanics 33, 531–542.

Herzog, W., Leonard, T.R., 2002. Force enhancement following stretching of skeletal muscle: a new mechanism. Journal of Experimental Biology 205, 1275–1283.

Herzog, W., Leonard, T.R., Wu, J.Z., 2000. The relationship between force depression following shortening and mechanical work in skeletal muscle. Journal of Biomechanics 33, 659–668.

Hisey, B., Leonard, T.R., Herzog, W., 2009. Does residual force enhancement increase with increasing stretch magnitudes? Journal of Biomechanics 42, 1488–1492.

Josephson, R.K., Stokes, D.R., 1999. Work-dependent deactivation of a crustacean muscle. Journal of Experimental Biology 202, 2551–2565.

Kadaba, M.P., Ramakrishnan, H.K., Wootten, M.E., 1990. Measurement of lower extremity kinematics during level walking. Journal of Orthopaedic Research 8, 383–392.

Kosterina, N., Westerblad, H., Lannergren, J., Eriksson, A., 2008. Muscular force production after concentric contraction. Journal of Biomechanics 41, 2422–2429.

Lee, H.D., Herzog, W., Leonard, T., 2001. Effects of cyclic changes in muscle length on force production in in-situ cat soleus. Journal of Biomechanics 34, 979–987.

Marechal, G., Plaghki, L., 1979. The deficit of the isometric tetanic tension redeveloped after a release of frog muscle at a constant velocity. Journal of General Physiology 73, 453–467.

McGowan, C.P., Kram, R., Neptune, R.R., 2009. Modulation of leg muscle function in response to altered demand for body support and forward propulsion during walking. Journal of Biomechanics 42, 850–856.

McGowan, C.P., Neptune, R.R., Herzog, W., 2010. A phenomenological model and validation of shortening-induced force depression during muscle contractions. Journal of Biomechanics 43, 449–454.

Meijer, K., Grootenboer, H.J., Koopman, H.F., van der Linden, B.J., Huijing, P.A., 1998. A Hill type model of rat medial gastrocnemius muscle that accounts for shortening history effects. Journal of Biomechanics 31, 555–563.

Neptune, R.R., Clark, D.J., Kautz, S.A., 2009. Modular control of human walking: a simulation study. Journal of Biomechanics 42, 1282–1287.

Neptune, R.R., Wright, I.C., Van Den Bogert, A.J., 2000. A method for numerical simulation of single limb ground contact events: application to heel–toe running. Computer Methods in Biomechanics and Biomedical Engineering 3, 321–334.

Peterson, D.R., Rassier, D.E., Herzog, W., 2004. Force enhancement in single skeletal muscle fibres on the ascending limb of the force–length relationship. Journal of Experimental Biology 207, 2787–2791.

Rankin, J.W., Richter, W.M., Neptune, R.R., 2011. Individual muscle contributions to push and recovery subtasks during wheelchair propulsion. Journal of Biomechanics 44, 1246–1252.

Voigt, M., Simonsen, E.B., Dyhre-Poulsen, P., Klausen, K., 1995. Mechanical and muscular factors influencing the performance in maximal vertical jumping after different prestretch loads. Journal of Biomechanics 28, 293–307.

Williams, T.L., 2010. A new model for force generation by skeletal muscle, incorporating work-dependent deactivation. Journal of Experimental Biology 213, 643–650.

Woltring, H.J., 1978. A FORTAN package for generalized cross-validatory spline smoothing and differentation. Advances in Engineering Software 8, 104–113.

Zajac, F.E., 1989. Muscle and tendon: properties, models, scaling, and application to biomechanics and motor control. Critical Reviews in Biomedical Engineering 17, 359–411.